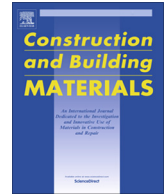




Contents lists available at ScienceDirect

# Construction and Building Materials

journal homepage: [www.elsevier.com/locate/conbuildmat](http://www.elsevier.com/locate/conbuildmat)



## Review

# Geocell reinforced foundation beds-past findings, present trends and future prospects: A state-of-the-art review



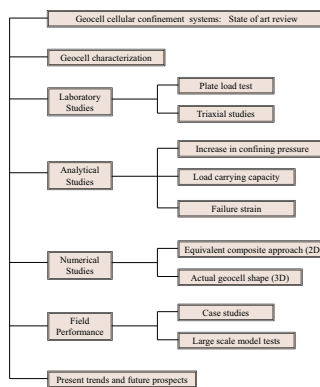
A. Hegde

Department of Civil and Environmental Engineering, Indian Institute of Technology Patna, 801103, India

### HIGHLIGHTS

- Presented current state-of-the-art regarding geocells.
- Reviewed past studies related to geocells.
- Documented studies related to field performance of geocells.
- Discussed future prospects of the geocells in geotechnical engineering.
- Geocell found to be very promising ground reinforcement technique.

### GRAPHICAL ABSTRACT



### ARTICLE INFO

**Article history:**

Received 13 November 2016  
 Received in revised form 21 June 2017  
 Accepted 31 July 2017

**Keywords:**

Geocells  
 Plate load test  
 Soft clay  
 Foundations  
 Simulations  
 Pavements

### ABSTRACT

In the last few years, the use of geocell reinforcements in various infrastructural projects has gained importance due to its positive benefits. This paper reviews the developments and state-of-the-art pertinent to geocell research and field practices. The geocell studies covering, experimental, numerical, analytical and field performances have been reviewed. Characterization of the geocell has been discussed in detail. The field investigations of the test sections and the performance of the in-service geocell supported structures have been reviewed. A note has been presented on current research trends and the future prospects. A summary of the past research findings has been presented with a discussion on the research gaps in the subject area. It is evident from the past studies that the geocell is evolving as a promising sustainable ground reinforcement technique. Due to an increased use of geocells in the infrastructure projects, there exists an expansive scope for further research to understand the material better.

© 2017 Elsevier Ltd. All rights reserved.

### Contents

1. Introduction . . . . .	659
2. Characterization of the geocells . . . . .	660
3. Experimental Studies . . . . .	661

Abbreviations: CTE, Coefficient of Thermal Expansion; ECA, Equivalent composite Approach; ESCR, Environmental Stress–Cracking Resistance; HDPE, High-density polyethylene; NPA, Novel Polymeric Alloy; OIT, Oxidative induction Time; PRS, Percentage reduction in the footing settlement.  
 E-mail address: [ahegde@iitp.ac.in](mailto:ahegde@iitp.ac.in)

**Nomenclature**

$B$	footing width (m)	$R_a$	surface roughness ( $\mu\text{m}$ )
$C_r$	apparent cohesion (kPa)	$S_o$	settlement of the unreinforced foundation bed (m)
$D$	equivalent diameter of the geocell pocket opening (m)	$S_r$	settlement of the reinforced bed (m)
$D_r$	depth of the reinforcement (m)	$T$	tensile strength of the basal geogrid material (kN/m)
$E_i$	initial tangent modulus of the geocell layer (kPa)	$\alpha$	horizontal angle of the tensional force (degrees)
$I_f$	improvement factors (dimensionless)	$\beta$	load dispersion angle (degrees)
$K_p$	coefficient of passive earth pressure (dimensionless)	$\sigma_1$	normal stress (kPa)
$K_r$	Young's modulus parameter of the geocell-reinforced sand (dimensionless)	$\sigma_3$	confining stress (kPa)
$K_e$	Young's modulus parameter of the unreinforced sand (dimensionless)	$\sigma_h$	hoop stress (kPa)
$k_1, k_2, k_3$	resilient modulus parameters (dimensionless)	$\Delta\sigma_3$	increase in the confining stress (kPa)
$M$	secant stiffness of the geocell (kN/m)	$\zeta_a$	axial strain (percentage)
$M_r$	resilient modulus (kPa)	$\psi$	dilation angle (degrees)
$n$	modulus exponent (dimensionless)	$\theta$	bulk stress (kPa)
$N_{\text{limit}}$	limiting number of cycles (dimensionless)	$\tau_{\text{oct}}$	octahedral shear stress (kPa)
$P$	active earth pressure (kPa)	$\nu_g$	Poisson's ratio of geocell (dimensionless)
$p_a$	atmosphere pressure (kPa)	$\varepsilon_h$	hoop strain (percentage)
$q_r$	bearing pressure of the reinforced bed (kPa)	$\varepsilon_3$	percentage radial strain (percentage)
$q_o$	bearing pressure of unreinforced bed (kPa)	$\varepsilon_c$	circumferential strain (percentage)
$q_{\text{ult}}$	ultimate bearing capacity (kPa)	$\varepsilon_l$	volumetric strain (percentage)

3.1.	Laboratory model tests	661
3.2.	Triaxial studies	662
4.	Analytical studies	662
4.1.	Increase in confining pressure	662
4.2.	Load carrying capacity	665
4.3.	Failure stresses and strains	665
5.	Numerical studies	666
5.1.	Equivalent composite approach (ECA)	666
5.2.	Actual shape 3D model	666
6.	Field performance	668
6.1.	Case studies	668
6.2.	Field tests and large scale model tests	668
7.	Summary of the past studies	670
8.	Present research trends	671
9.	Future prospects	672
10.	Conclusions	672
	Acknowledgement	672
	References	672

**1. Introduction**

Due to the rapid urbanization in the 21st century, construction in weak ground has become inevitable. In recent years, ground improvement techniques like vibro stone columns and prefabricated vertical drains have gained the popularity for their wide range of application in soft soils. However, engineers and scientists are constantly looking for new techniques which are faster and cheaper to the traditional techniques. As a result of this, geocell applications are increasing at a rapid rate. Nowadays, geocells are being widely used in many geotechnical engineering applications. Geocells are the cost-effective, sustainable materials used to enhance the performance of soft soil. These are three-dimensional in shape and are made up of ultrasonically welded high strength polymers or the polymeric alloy such as Polyethylene, Polyolefin etc. Due to its 3-dimensional nature, geocell offers all-round confinement to the encapsulated soil, which leads to the overall improvement in the performance of the foundation beds [36].

Geocell was originally developed by the US army corps of engineers in the early 1970s for military applications. Later on, many researchers in the past have contributed to the development of the geocell technology. The majority of the past studies were laboratory in nature and these studies were carried out mainly to understand the efficacy of the geocells in enhancing the performance of the soil beds (e.g. [79,10,68,20,21,22,23,83,93,66,24,25,32,36,37]). Mid 1990 onward, numerical simulation techniques were adopted to understand the behaviour of the geocells. Over the years, many researchers have contributed in enhancing the knowledge about the geocells by means of the numerical simulations (e.g. [67,12,63,29,66,80,95,32,36,38,39,40]). Based on the experimental and numerical simulation observations, many researchers have developed the analytical formulations for calculating the bearing capacity of the geocell reinforced foundation beds (e.g. [58,74,99,9,85,42]). The latest trend is to carry out the large scale model tests or the actual field tests to understand the behaviour of the geocells (e.g. [27,31,96,89,70]). Further, the actual

field application of the geocell has been documented by few researchers as case histories (e.g. [19,56,85]).

Geocell are considered as cost effective, environmental friendly, durable and easy to use. It can be used in all weather conditions without any major maintenance. General applications include foundations, embankments, pavements, earth retaining structures and erosion control. Nowadays, the geocell applications are growing at the rapid rate due to its proven advantages over traditional techniques. As the geocell applications are growing at the rapid rate, it is very high time to summarize the past findings and analyse the future prospects of the geocell technology. This manuscript deals with the comprehensive review of the literatures related to geocell cellular confinement system. The emphasis is given to the recent literatures, in order to highlight the latest development in the field of cellular confinement systems. The available literatures on the geocells are categorically divided into 4 major sections namely, laboratory model studies, analytical studies, numerical studies, case studies cum full scale studies. The idea is to present the reader with the summary of the past studies, current state of art and the scope of the future research directions. Fig. 1 represents the outline of the review carried out in the present manuscript.

## 2. Characterization of the geocells

A detailed characterization of any material is essential before its use. The general geocell characterization includes the determination of its cell dimensions, aspect ratio, strip thickness, density,

surface area, tensile strength and seam strength. In addition, the knowledge about advanced properties of the geocells such as creep reduction factors, durability to UV Degradation and allowed strength for design of 50 years are essential in the design of the geotechnical structures involving geocells. The design of the geocell for extreme environment and varying temperature conditions demands the determination of the properties like Environmental Stress-Cracking Resistance (ESCR), Coefficient of Thermal Expansion (CTE) and Oxidative induction Time (OIT). In the load support applications, surface characteristics of the geocells play an important role in deciding its performance. Generally, the geocell possesses a unique cup shaped texture on its surface. Fig. 2a shows the SEM image of the surface texture. These textures are responsible for the roughness of the surface. The surface roughness is responsible for the interface friction between the material and the soil. Higher the surface roughness, higher is the interface friction. The surface roughness ( $R_a$ ) can be quantified using the optical profilometer [37]. Fig. 2b shows the typical surface roughness profile of the geocell material. When subjected to varying degrees of temperature, moisture, pressure, or other stress, the geocells must retain their original dimensions (dimensional stability). If the geocell loses its original dimensions, it can weaken the confinement and compaction leading to degradation or failure of a structure. The simplest way of measuring the dimensional stability is by means of the Coefficient of Thermal Expansion (CTE). The low value of the CTE indicates the high dimensional stability. The recent Neoloy geocells made from reinforcing the nano-fibers in a polyolefin

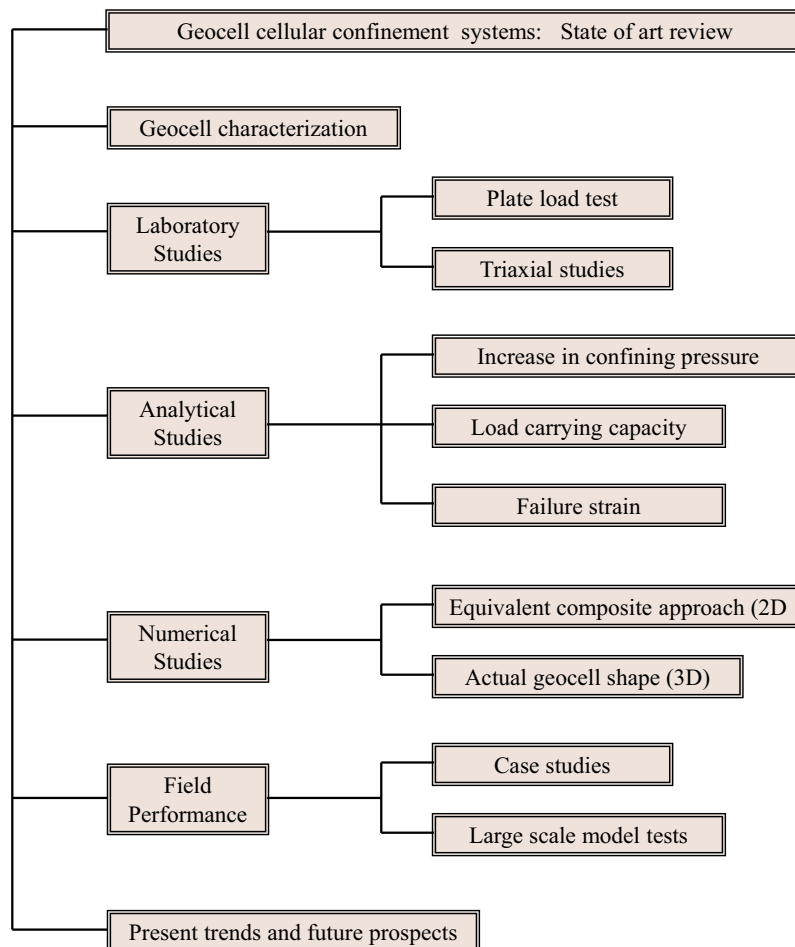


Fig. 1. Research review outline.

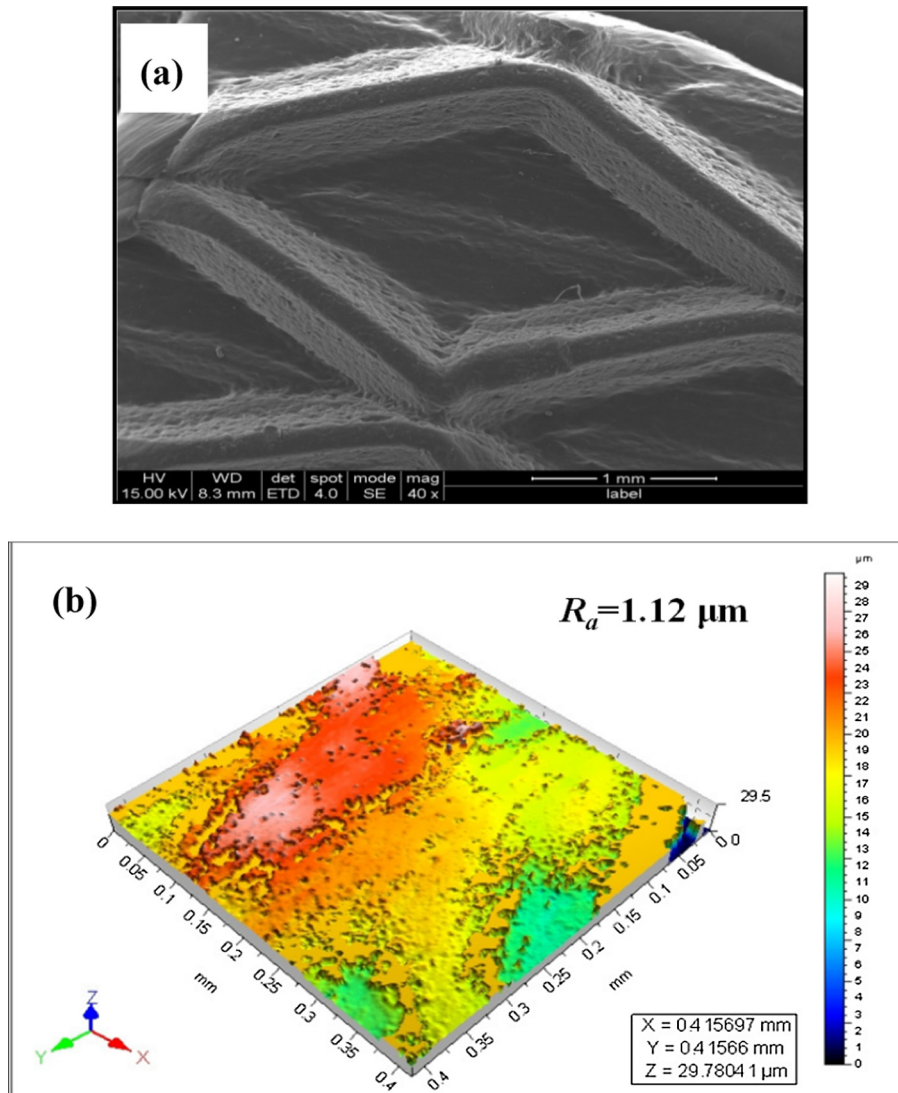


Fig. 2. Geocell surface characteristics: (a) SEM image (sourced from Hegde [35]); (b) roughness profile (sourced from Hegde and Sitharam [37]).

are chemically very stable and are having the CTE less than 80 Ppm/ $^{\circ}\text{C}$ . Table 1 lists the typical properties of the geocells and the reference standards used in the determination of the same.

### 3. Experimental Studies

#### 3.1. Laboratory model tests

The majority of the previous researchers have used the laboratory model tests to study the efficacy of the geocells. Fig. 3a–b shows the typical experimental setup used in these studies. The typical test setup consisted of a tank connected to the hydraulic jack to apply the load. The model foundation bed was prepared in the tank and load was applied via steel plate. The dial gauges and load cells were used to measure the displacement of the bed and the applied load respectively. Initially, Rea and Mitchell [79] studied the behaviour of the circular footing resting on the geocell reinforced sand bed. In their study, the geocell was prepared using the paper. Subsequently, many researchers have used the geocells made from the different material in their study viz. polypropylene, polyester and high density polyethylene (HDPE) etc. The studies conducted in the recent past have used the high

strength Neoloy geocells [31,96,32,36,37]. The Novel Polymeric Alloy (NPA), also known as Neoloy, is a polymeric alloy composed of polyolefin and thermoplastic engineering polymer. These geocells are known for high strength and durability. Fig. 4a–d shows the photographs of the different type of the geocells used in the past studies.

In addition to different type of geocells, the different shapes of the footing were also used by the researchers in the past. Table 2 summarizes important laboratory studies related to geocell reinforced foundation beds. Fig. 5 shows the pictorial representation of the variable parameters used in Table 2.

The majority of these reported studies have focussed on evaluating the overall performance of the foundation bed in the presence of geocells. The effect of geocell geometry, foundation bed properties, infill materials and the effect of basal geogrid were also studied. The overall performance of the foundation bed was quantified in terms of the increase in bearing capacity and reduction in the settlement. These parameters were expressed in terms of dimensionless parameters, namely, bearing capacity improvement factors ( $I_f$ ) and the percentage reduction in the footing settlement (PRS) respectively [20,21,22,82,83,32]. The bearing capacity improvement factor is defined as,

**Table 1**  
Typical properties of the NPA geocells (Data Courtesy of PRS Mediterranean, Ltd.)

Properties	Values	Units	Test methods
Density	0.95	g/cm <sup>3</sup>	ASTM D1505 [8]
Strip thickness	1.53 (±10%)	mm	ASTM D5119 [1]
Tensile strength	>20	N/mm	PRS method <sup>a</sup>
Diameter of the hole on the surface	10	mm	N/A
Percentage open area on the surface	16	%	N/A
Allowed strength for design of 50 years	>8	kN/m	ASTM D6992 [7] <sup>b</sup>
Creep reduction factor	>2.7		ASTM D6992 [7] <sup>c</sup>
Environmental Stress-Cracking Resistance (ESCR)	>3000	hr	ASTM D1693 [6]
Coefficient of Thermal Expansion (CTE)	<80	Ppm/°C	ISO 11359-2 [54] ASTM E831 [3] <sup>d</sup>
Durability to UV Degradation	>250	Minutes	ASTM D5885 [2] (High pressure oxidative induction time (HPOIT) at 150 °C, 3500 kPa)
Oxidative induction Time (OIT)	>100	min	ISO 11357-6 [52], ASTM D3895 [4] (OIT at 200 °C, 25 kPa)
Flexural Storage Modulus at sample temp:30 °C45 °C60 °C75 °C	>750 >650 >550 >300	MPA	ISO 6721-1 [53] ASTM E2254 [5]

<sup>a</sup> Test sample cut from cell seam to seam measured at strain rate 20%/min, 23 °C.

<sup>b</sup> Allowed strength to reach 10% creep strain max for 50 years at 23 °C.

<sup>c</sup> Creep (deformation) reduction factor for 50 years at 23 °C.

<sup>d</sup> CTE measurement range from –30 °C to +30 °C.

$$I_f = \frac{q_r}{q_o} \quad (1)$$

where  $q_r$  is the bearing pressure of the reinforced bed at a particular settlement and  $q_o$  is the bearing pressure of unreinforced bed at the same settlement. Bearing capacity improvement factor is similar to the bearing capacity ratio reported by Binquet and Lee [15]. When the ratio is beyond the ultimate bearing capacity of the unreinforced bed, the ultimate bearing capacity ( $q_{ult}$ ) is used instead of  $q_o$ . The improvement factor depends on the various parameters such as, foundation soil properties, geocell material, infill soil properties and the aspect ratio of the geocells. Further, for a particular type of geocell and the soil, the improvement factor even varies with the settlement of the bed. On an average, the improvement factor for Neoloy geocells varies in the range of 4–6 [32]. However, some researchers have reported the values even up to 9 for different test bed conditions. Table 3 summarizes the values of the improvement factor reported by the various researchers for the different test conditions.

Similarly, the PRS is defined as,

$$PRS = \left( \frac{S_o - S_r}{S_o} \right) \times 100 \quad (2)$$

where  $S_o$  is settlement of the unreinforced foundation bed corresponding to its ultimate bearing capacity and  $S_r$  is the settlement of the reinforced bed corresponding to the ultimate bearing capacity of the unreinforced bed. Generally, the double tangent method is used to estimate the ultimate load bearing capacity. In this method, the ultimate bearing capacity is determined by drawing the two tangents; one at the early part of the pressure settlement curve and the another at the latter part. Hegde and Sitharam [36] reported the PRS value more than 70% in the clay bed reinforced with the geocells.

### 3.2. Triaxial studies

The improvement in the strength and the stiffness of the soil reinforced with the geocells can also be studied by means of the triaxial tests. Bathurst and Karpurapu [11] carried out a series of large scale triaxial tests on 200 mm high isolated geocell specimen. Test results indicated the drastic improvement in the apparent

cohesion with geocell reinforcement. Rajagopal et al. [77] also performed triaxial compression tests on granular soil encased in single and multiple geocells. Both geocell reinforced and unreinforced samples exhibited same frictional strength, but significant increase in apparent cohesion ( $C_r$ ) was observed in the reinforced case as shown in Fig. 6. In the figure, the small circle refers to the Mohr circle of the unreinforced soil. Due to the provision of geocell reinforcement, the confining stress increases from  $\sigma_3$  to  $\sigma_3 + \Delta \sigma_3$ . Due to which the ultimate normal stress increases to  $\sigma_1$  from  $\sigma_{1u}$ . The intermediate circle in the figure indicates the Mohr circle corresponding to this state. The same ultimate stress can also be represented with the larger Mohr circle which has a confining pressure of  $\sigma_3$  an apparent cohesion of  $c_r$  [77]. Researchers observed that the geocell reinforcement imparts apparent cohesive strength even to the cohesionless soil. Further, Zhang et al. [97] opined that inclusion of 3D reinforcement increases both apparent cohesion and the angle of internal friction of the soil. Chen et al. [18] carried out the triaxial compression tests on the geocell reinforced sand. In their study, the researchers have used the different shape of the geocells viz. circular, rectangular and the hexagonal. Out of all the tested shapes of the geocells, the circular shape was found most effective in increasing the apparent cohesion. Table 4 summarizes the past research activities related to triaxial studies on the geocells.

## 4. Analytical studies

### 4.1. Increase in confining pressure

The increase in the confining pressure due to the provision of the geocell can be estimated using the formulations provided in the literature. There are separate equations available for the calculation of the increase in the confining pressure in case of the static and cyclic loading conditions. Bathurst and Karpurapu [11] and Rajagopal et al. [77] provided the formulation for the static loading conditions. The formulation for the cyclic loading conditions has been provided by Yang and Han [94] and Indraratna et al. [51].

Bathurst and Karpurapu [11] reported that the geocell confinement of sand induces the apparent cohesion while the friction angle remains constant. As suggested by Rajagopal et al. [77], the induced apparent cohesion of the geocell-soil composite layer can be calculated using the Eqs. (3) and (4).

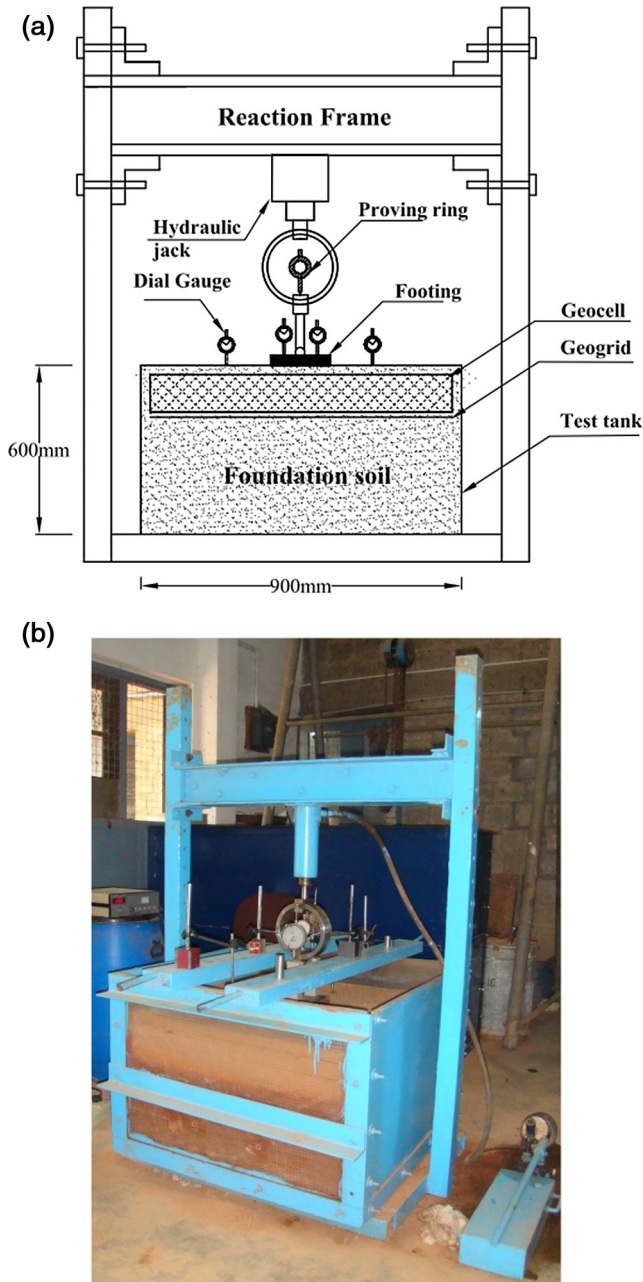


Fig. 3. Test setup: (a) schematic view (sourced from Hegde and Sitharam [39]); (b) photographic view.

The increase in the confining pressure ( $\Delta\sigma_3$ ) on the soil due to the presence of geocell is given by,

$$\Delta\sigma_3 = \frac{2M}{D} \left[ \frac{1 - \sqrt{1 - \xi_a}}{1 - \xi_a} \right] \quad (3)$$

where  $M$  is the secant modulus of the geocell material calculated corresponding to the axial strain of  $\xi_a$  in the tensile stress-strain response;  $D$  is the equivalent diameter of the geocell pocket opening. The increment in the apparent cohesion ( $C_r$ ) due to the increase in the confining pressure can be given by,

$$C_r = \frac{\Delta\sigma_3}{2} \sqrt{K_p} \quad (4)$$

where,  $K_p$  is the coefficient of passive earth pressure. The above equation was actually originated from the rubber membrane theory developed by Henkel and Gilbert [45] to correct the effects of stiff rubber membrane in triaxial tests. The equivalent stiffness of the geocell-soil composite can be related to the stiffness of the unreinforced soil, secant modulus of the geocell material and the interaction parameter (which represents the interaction, in case of multiple cells) as suggested by Madhavi Latha [62] below.

$$K_r = K_e + 200M^{0.16} \quad (5)$$

where  $K_r$  is the Young's modulus parameter of the geocell-reinforced sand and  $K_e$  is the Young's modulus parameter of the unreinforced sand. The Young's modulus parameter ( $K_e$ ) in the Eq. (5) corresponds to the modulus number in the hyperbolic model proposed by Duncan and Chang [26]. The equivalent initial tangent modulus of the geocell layer is then determined using the equation suggested by Janbu [55] to relate the stiffness of the soil to the confining pressure as given below.

$$E_i = K_r P_a \left( \frac{\sigma_3}{P_a} \right)^n \quad (6)$$

where  $E_i$  is the initial tangent modulus of the geocell layer,  $\sigma_3$  is the confining pressure acting at the midlevel of the geocell layer,  $P_a$  is the atmospheric pressure,  $K_r$  is the Young's modulus parameter of geocell layer determined using Eq. (5) and  $n$  is the modulus exponent of the unreinforced soil.

Yang and Han [94] proposed an equation to determine the increase in the confining pressure ( $\Delta\sigma_3$ ) due to the provision of the geocell subjected to repeated loading. Researchers have formulated the equation based on the repeated load triaxial test results as represented below.

$$\Delta\sigma_3 = \frac{M}{D} \left[ -\frac{\Delta\sigma_3}{M_{r1}} + \frac{\sigma_1 - (\sigma_3 + \Delta\sigma_3)}{M_{r2}} \right] \times \left( \frac{\epsilon_0}{\epsilon_r} \right) e^{(-\rho/N_{limit})^\beta} \left( \frac{1 + \sin \psi}{1 - \sin \psi} \right) \quad (7)$$

where  $D$  is the diameter of the sample;  $M$  is the tensile stiffness of the geocell (in force/length);  $\sigma_3$  is the confining stress in the triaxial test;  $\sigma_1$  is the vertical stress in the triaxial test;  $\psi$  is the dilation angle;  $M_{r1}$  is the resilient modulus during the stage at which confining stress was increased from  $\sigma_3$  to  $\sigma_3 + \Delta\sigma_3$ .  $M_{r2}$  is the resilient modulus during the stage at which confining stress was increased from  $\sigma_3$  to  $\sigma_3 + \Delta\sigma_3$ ;  $(\epsilon_0/\epsilon_r)$ ,  $\rho$  and  $\beta$  are the permanent deformation parameter of the granular material.  $N_{limit}$  is the limiting number of cycles. The resilient modulus ( $M_r$ ) is calculated using the equations below.

$$M_r = k_1 P_a \left( \frac{\theta}{P_a} \right)^{k_2} \left( \frac{\tau_{oct}}{P_a} + 1 \right)^{k_3} \quad (8)$$

where  $k_1$ ,  $k_2$ , and  $k_3$  are resilient modulus parameters of the material;  $p_a$  is atmospheric pressure;  $\theta$  is the bulk stress and  $\tau_{oct}$  is the octahedral shear stress. The resilient modulus  $M_{r1}$  is determined using the Eq. (8) with

$$\theta = \sigma_3 + 2(\sigma_3 + \Delta\sigma_3) \quad (9)$$

$$\tau_{oct} = \frac{\sqrt{2}}{3} \Delta\sigma_3 \quad (10)$$

The resilient modulus  $M_{r2}$  is determined using the Eq. (8) with

$$\theta = \sigma_1 + 2(\sigma_3 + \Delta\sigma_3) \quad (11)$$

$$\tau_{oct} = \frac{\sqrt{2}}{3} [\sigma_1 - (\sigma_3 + \Delta\sigma_3)] \quad (12)$$

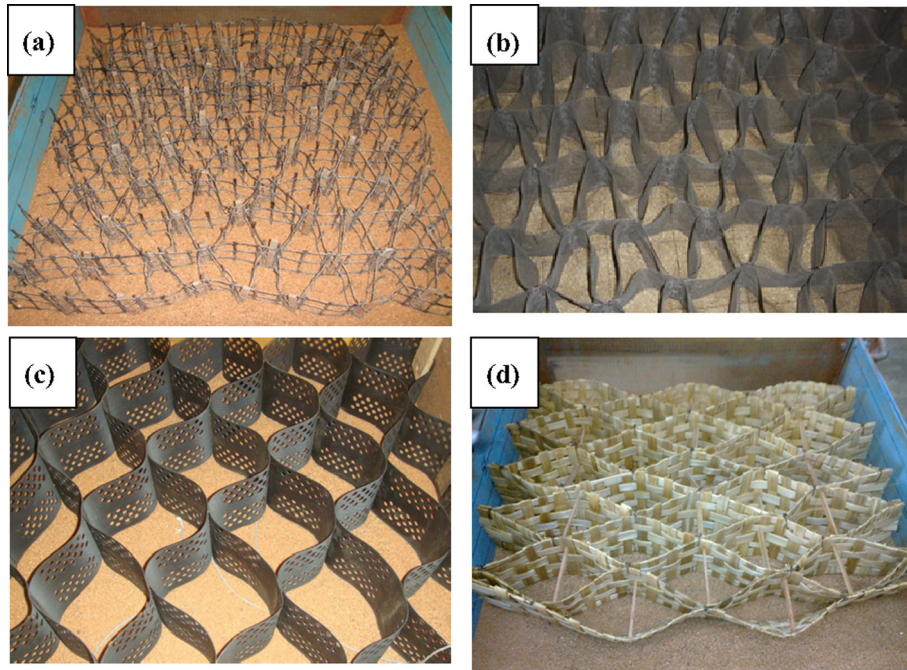


**Fig. 4.** Geocells made from different materials: (a) geogrid<sup>1</sup>; (b) geonet<sup>2</sup>; (c) neoloy<sup>1</sup>; (d) bamboo<sup>1</sup> (<sup>1</sup>sourced from Hegde and Sitharam [44]; <sup>2</sup>sourced from Madhavi Latha and Somwanshi [66]).

**Table 2**  
Summary of the experimental studies related to geocell supported footing subjected to static loading.

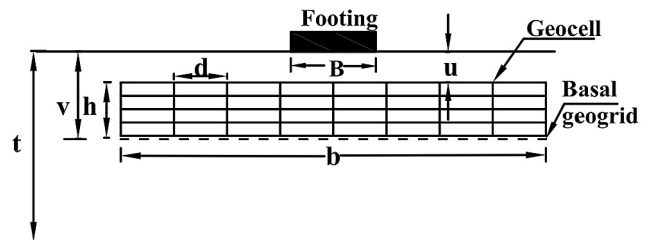
Researchers	Footing shape	Foundation soil	Infill material	Geocell material	Parameter varied
Rea and Mitchel [79]	Circular	Sand	Rubber/sand	Paper	$D/b$ ; $b/h$ ; $K$
Bathurst and Jarrett [10]	Strip	Peat	Crushed aggregate	Polyethylene	$t$
Mandal and Gupta [68]	Strip	Soft marine clay	Sand	Geotextiles	$h/B$
Krishnaswamy et al. [57]	Strip	Soft soil	Soft soil	Geogrids	$GM$
Dash et al. [20]	Strip	Sand	Sand	Geogrids	$b/B$ ; $h/B$ ; $u/B$ ; $d/B$
Dash et al. [22]	Circular	Silty clay	Sand	Geogrids	$b/D$ ; $h/D$ ; $BG$
Dash et al. [23]	Strip	Sand	Sand	Geogrids	$BG$
Sitharam and Sireesh [83]	Circular	Sand and clay	Sand and moist clay	Geogrids	$b/D$ ; $h/D$ ; $u/D$
Sitharam and Sireesh [84]	Circular	Sand and clay	Sand	Geogrid	$h/D$ ; $BG$
Thallak et al. [93]	Circular	Silty clay	Silty clay	Geogrids	$b/D$ ; $h/D$ ; $u/D$
Madhavi Latha and Somwanshi [66]	Square	Sand	Sand	Geogrids and geonets	$GM$
Sireesh et al. [81]	Circular	Clay	Sand	Geogrids	$b/D$ ; $h/D$ ; $RD$
Dash [24]	Strip	Sand	Sand	Geogrids	$RD$
Pokharel et al. [75]	Circular	Firm base	Sand	HDPE & Neoloy	$h$ , $IM$ , $GS$ , $GM$
Han et al. [30]	Circular	Firm base	Sand, aggregate, quarry waste	Neoloy	$IM$
Dash [25]	Strip	Sand	Sand	Geogrids	$GM$
Hegde and Sitharam [32]	Square	Sand and Cay	Sand	Neoloy	$BG$
Hegde and Sitharam [36]	Square	Cay	Sand, clay and aggregate	Neoloy	$IM$
Hegde and Sitharam [37]	Square	Cay	Sand	Neoloy, Bamboo	$GM$

B: Footing width; D = footing diameter; h = geocell height; d = geocell pocket diameter; u = geocell depth; b = geocell width; t = subgrade thickness; K = subgrade thickness; GM = geocell material; GS = geocell shape; IM = infill material; RD = Relative density of bed; BG = Basal geogrid.

Similarly, Indraratna et al. [51] proposed equation for determining the additional confinement due to the provision of geocell subjected to cyclic loading. The additional confinement offered by the geocell was computed using the hoop tension theory. The following equation was given.

$$\Delta\sigma_3 = \frac{2M}{D} \frac{[(1 - \nu_g)(k + \nu_g)]}{(1 + \nu_g)(1 - 2\nu_g)} (-\epsilon_3) \tag{13}$$

where  $\Delta\sigma_3$  is additional confining stress in each pocket;  $D$  is the diameter of an equivalent circular area of the geocell pocket;  $M$  is the mobilized modulus of the geocell;  $\nu_g$  is the Poisson's ratio of geocell;  $k$  is the ratio between  $\epsilon_c$  and  $\epsilon_3$ ;  $\epsilon_3$  is the percentage radial strain;  $\epsilon_c$  percentage circumferential strain.



- b width of geocell
- B width of footing
- d pocket size of geocell
- h height of geocell
- t thickness of clay bed
- u depth of geocell
- v depth of geogrid

**Fig. 5.** Schematic representation of the parameters described Table 2.

**Table 3**

Value of the improvement factor reported by the various researchers.

Researchers	Type of reinforcement	Type of soil bed	Type of infill soil	Improvement factors (max)
Dash et al. [20]	Geocells made from geogrid	Sand (RD = 70%)	Sand	8
Dash et al. [22]	Geocells made from geogrid	Clay( $C_u = 3.1$ kPa)	Sand	5.4
Sitharam and Sireesh [83]	Geocells made from geogrid	Sand (RD = 70%)	Sand	9.5
Sitharam and Sireesh [83]	Geocells made from geogrid	Clay ( $C_u = 5.6$ kPa)	Sand	5.5
Madhavi Latha and Somwanshi [66]	Geocells made from geogrid	Sand (RD = 70%)	Sand	4.75
Sireesh et al. [81]	Geocells made from geogrid	Clay( $C_u = 10$ kPa)	Sand	4.9
Hegde and Sitharam [32]	Neoloy geocell	Sand (RD = 70%)	Sand	3.2
Hegde and Sitharam [32]	Neoloy geocell	Clay( $C_u = 5$ kPa)	Sand	6
Hegde and Sitharam [36]	Neoloy geocell with basal geogrid	Clay( $C_u = 10$ kPa)	Silty clay	8
Hegde and Sitharam [36]	Neoloy geocell with basal geogrid	Clay( $C_u = 10$ kPa)	Sand	10
Hegde and Sitharam [36]	Neoloy geocell with basal geogrid	Clay( $C_u = 10$ kPa)	Aggregate	12

RD: Relative density;  $C_u$  = Undrained cohesion.

#### 4.2. Load carrying capacity

Koerner [58] proposed the analytical solution to estimate the bearing capacity of the geocell reinforced foundation beds. This method attributes the increase in bearing capacity of the geocell reinforced soil to the lateral resistance effect developed due to the interfacial friction between soil and cell wall. Presto [74] had developed a bearing capacity equation for the geocell reinforced sand. The equation was developed based on the empirical design methods of the unpaved road over the soft subgrade. Zhao et al. [98] opined that the increase in the bearing capacity of the geocell reinforced soil is mainly due to three mechanisms: (a) lateral resistance effect, (b) vertical stress dispersion effect and (c) membrane effect. Further, Zhang et al. [99] proposed simple bearing capacity equations for geocell supported embankment over the soft soil. This method considers only vertical stress dispersion mechanism and the membrane mechanism. Similarly, Sitharam and Hegde [85] proposed a method to estimate the increase in the load carrying capacity of the geocell reinforced soft clay beds by considering all the three mechanisms proposed by Zhao et al. [98]. This model is based on the hypothesis that the lateral resistance effect and the vertical stress dispersion effect are contributed by the geocell while the membrane effect is originated by virtue of basal geogrid.

Koerner [58] opined that the lateral resistance effect originate due to the interaction between the geocell surface and the infill soil. The interaction leads to the development of the additional shear strength at the interface, which will enhance the bearing capacity of the geocell reinforce soil. The schematic view of the lateral resistance mechanism is shown in Fig. 7a. The vertical stress dispersion mechanism is also called as the wide slab mechanism. This mechanism was first observed by Binquet and Lee [15]. Schlosser et al. [86] extended this mechanism to the strip footing resting on the reinforced soil beds. Subsequently, many researchers have reported the wide slab mechanism in their studies [46,47,87]. In addition, the presence of a wide slab mechanism in the geocell reinforced foundation bed was justified by the findings of Dash et al. [20,21], Sitharam and Sireesh [82,83] through 1-g model tests. They observed that the interconnected cells form a panel that acts like a large slab that spreads the applied load over an extended area leading to the overall improvement in the performance of the foundation soil. Fig. 7b is the schematic representation of the vertical stress dispersion mechanism in the geocell reinforced foundation beds. Footing of width  $B$  resting on the geocell reinforcement behaves as if the footing of width  $B + \Delta B$  resting on soft soil at the depth of  $D_r$  (where  $D_r$  is the depth of the reinforcement) and  $\beta$  is the load dispersion angle that varies between  $30^\circ$  to  $45^\circ$ .

The membrane effect mechanism is contributed by the vertical component of the mobilized tensile strength of the planar reinforcement [99]. Sitharam and Hegde [85] observed that membrane

mechanism originated due to the resistance offered by the soil reinforcement to the bending. The schematic view of the membrane mechanism is shown in Fig. 7c. In the figure,  $T$  is the tensile strength of the basal geogrid material and  $\alpha$  is the horizontal angle of the tensional force  $T$ . When the vertical load is applied on the combination of the geocell and the geogrid, the deformed shape of geogrid is generally parabolic in nature. However, if the footing dimension is very small compared to the geogrid dimension, then it resembles the triangular shape as shown in Fig. 7c. Similarly, Avesani Neto et al. [9] also derived the bearing capacity equation for the soil reinforced with the geocells. In their formulation, the bearing capacity equation of the geocell reinforced soil was obtained summing up the bearing capacity of the unreinforced soil and the bearing capacity improvement caused by geocells. Researchers have considered three mechanisms, namely, confinement effect, stress dispersion effect and the membrane effect. The summary of the bearing capacity equations provided by different researches are presented in Table 5.

#### 4.3. Failure stresses and strains

When a vertical load is applied to the geocell-soil composite, the mobilization of horizontal stresses takes place in the infill material. The horizontal stress, thus developed imparts the active earth pressure on the cell wall. The active earth pressure on the cell wall generates Hoop stress within the wall and the passive earth pressure on the adjacent walls [27]. Hence, the confinement effect of the geocell is based on three main mechanisms: active earth pressure within loaded cell, passive earth pressure in the adjacent cells and the Hoop stress within the cell wall [27,38]. The different stresses developed in the geocell walls under the action of compression loads are shown in Fig. 8. The Hoop stress will lead to the deformation of the cell wall. The cell wall deformations can be measured in terms of Hoop strains and the volumetric strains. Hegde and Sitharam [38] developed the expression for the Hoop stress, Hoop strain and the volumetric strains in the geocell surface using the theory of thin cylinder formulations.

Fig. 9 represents the stresses acting on the surface of the deformed geocell as reported by Hegde and Sitharam [38]. The only half portion of the geocell was considered by the researchers in the formulation due to the symmetry.  $P$  is the active earth pressure exerted by the infill soil on the geocell wall. Researchers have considered the a small element of length,  $l$  on the periphery of the geocell, making an angle  $d\theta$  with the centre to obtain the expression for Hoop stress ( $\sigma_h$ ), Hoop strain ( $\epsilon_h$ ) and volumetric strain ( $\epsilon_v$ ). Table 6 lists the expression for the Hoop stress, Hoop strain and the volumetric strains in the geocell surface. These expressions can be used to evaluate the stresses and strains on the geocell. By knowing the possible load from the superstructure, basic physical parameters ( $d$  &  $t$ ) and elastic parameters ( $E$  &  $\mu$ ) of the geocell,

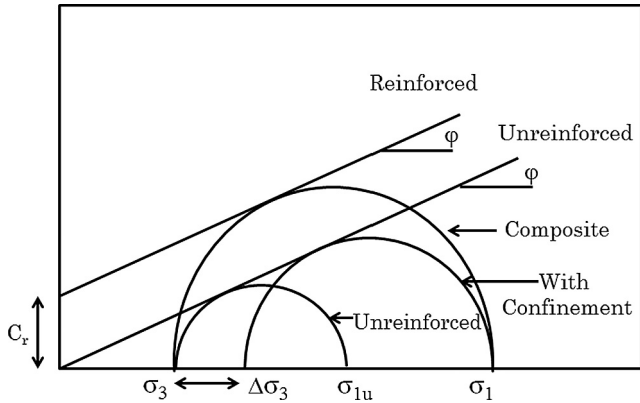


Fig. 6. Mohr circle for calculation of the apparent cohesion for geocell soil composite (figure reproduced from Rajagopal et al. [77]).

the stresses and strains on the geocell can be evaluated. The geocell design can then be optimized to keep these stresses and strains within desired limits of failure. The limiting strain value reported by the Hegde and Sitharam [38] was in the range 1.3%.

5. Numerical studies

5.1. Equivalent composite approach (ECA)

The equivalent composite approach (ECA) is the simplest method of modelling the geocells in the two dimensional framework. The ECA was adopted by many of the researchers in the past to model the geocells [66,32,69,36]. In this approach, the geocell

in-filled with sand is modelled as the composite soil layer with improved strength and stiffness parameters. The improved strength and elastic properties of the geocell-soil composite are determined using the formulation illustrated in the Section 4.1 using the Eqs. (3)–(6). Fig. 10a shows the typical ECA numerical model for geocells.

5.2. Actual shape 3D model

Though the ECA offers a simple way of modelling the geocells in 2-dimensional framework, it has certain limitations as reported by Hegde and Sitharam [39]. Firstly, it overestimates the bearing capacity of the geocell reinforced foundation beds. Also, it cannot handle the situation, if the combinations of reinforcements are provided e.g. combination of geocell and geogrid; which is very common practice in the field. In addition, the ECA is applicable only to the geocells with the aspect ratio in between 0.5 and 2.1 [66]. In order to overcome these limitations, more realistic approach of modeling the geocells has been practiced in the recent studies. The recent trend is to model the geocells in 3-dimensional framework by considering its actual shape. However, this approach is slightly complex due to the honeycomb shape of the geocells. Due to this reason, different researchers have used simplified shapes to the geocell pockets.

The numerical simulation of single cell geocell subjected to uniaxial compression was carried out by Han et al. [29] in  $FLAC^{3D}$ . Due to the difficulty in modeling the actual shape, the cell was modeled as the square box in their study. For similar reasons, Hegde and Sitharam [38] used the circular shaped pocket geometry in their study. Researchers observed the deviation in the experimental and numerical pressure-settlement response. The deviation in the result was attributed to the shape of the geocell pocket used

Table 4 Summary of triaxial studies related to the geocells.

Researchers	Specimen size	Geocell material/size/number of cells	Confining pressure
Bathrust and Karpurapu [11]	350 mm dia and 700 mm height	Polyethylene/200 mm dia/single cell with varying aspect ratio	10, 25, 50, 75 and 100 kPa
Rajagopal et.al [77]	100 mm in dia and 200 mm in height	Geotextile/varying dia/single as well as multiple	100, 150 and 200 kPa
Zhang et al. [97]	61.8 mm dia and 135 mm height	Galvanized iron sheet/4 cm dia/single and double	50, 100, 150 and 200 kPa
Chen et al. [18]	70 mm dia and 140 mm height; 150 mm dia and 300 mm height	High density Polyethylene (HDPE)/varying dia/single as well as multiple	50 kPa, 100 kPa and 200 kPa

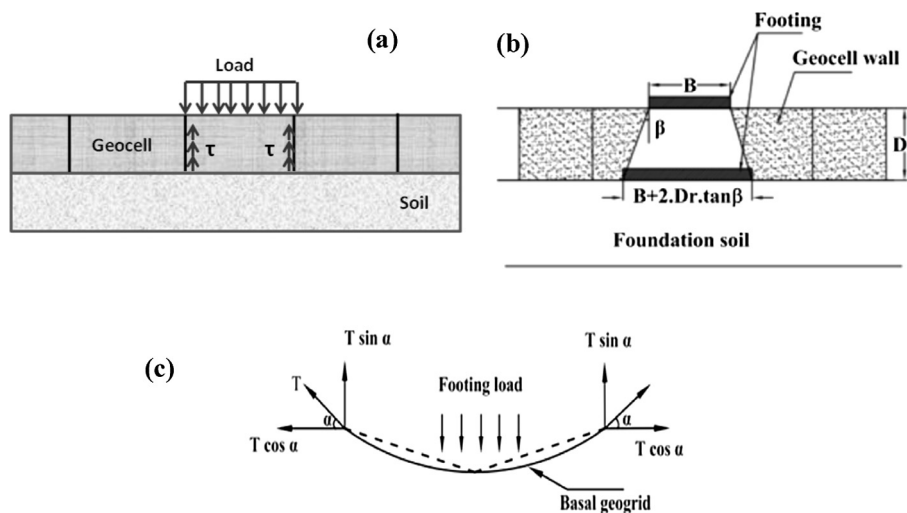


Fig. 7. Load carrying mechanisms: (a) Lateral resistance effect; (b) vertical stress dispersion<sup>1</sup>; (c) membrane mechanism<sup>1</sup> (<sup>1</sup>sourced from Sitharam and Hegde [85]).

**Table 5**  
Summary of the studies related to bearing capacity calculations of geocell reinforced soil.

Researchers	Mechanisms considered	Bearing capacity equations	Parameters
Koerner [58]	Lateral resistance effect	$P_r = 2p \tan^2(45 - \varphi/2) \tan \delta + cN_c S_c + qN_q S_q + 0.5\gamma B N_\gamma S_\gamma$	$P_r$ = bearing capacity of the reinforced soil (kPa); $p$ = applied pressure on geocell mattress (kPa) $\varphi$ = friction angle of the soil used to fill the geocell pockets (degrees) $\delta$ = interface shear angle between the cell wall and the filling soil (degrees) $c$ = cohesion of the soil (kPa) $q$ = surcharge load (kPa) $B$ = width of the applied pressure system (m) $\gamma$ = unit weight of the soil (kN/m <sup>3</sup> ) $N_c, N_q, N_\gamma$ = bearing capacity factors (dimensionless) $S_c, S_q, S_\gamma$ = shape factors (dimensionless)
Presto [74]	N/A	$P_r = 2 \frac{h}{d} k_a \sigma_{vm} \tan \delta + C_u N_c$	$P_r$ = bearing capacity of the reinforced soil (kPa); $h/d$ = geocell aspect ratio (dimensionless); $k_a$ = coefficient of active earth pressure (dimensionless); $\sigma_{vm}$ = average vertical stress (kPa); $\delta$ = interface shear angle between the cell wall and the filling soil (degrees) $C_u$ = subgrade shear strength (kPa); $N_c$ = bearing capacity coefficient (dimensionless);
Zhang et al. [99]	Vertical stress dispersion and membrane mechanisms	$P_r = p_s + \frac{2h_c \tan \theta_c}{b_n} p + \frac{2T \sin \alpha}{b_n}$	$P_r$ = bearing capacity of the reinforced soil (kPa); $p$ = applied pressure on geocell mattress (kPa) $b_n$ = width of the uniform load (m); $h_c$ = height of the geocell-reinforced cushion $\theta_c$ = dispersion angle of the geocell reinforcement (degrees) $T$ = tensile force in geocell reinforcement (kN/m) $\alpha$ = horizontal angle of the tensional force T (degrees)
Avesani Neto et al. [9]	Confinement effect, stress dispersion effect and the membrane effect	$P_r = P_u + 4 \frac{h}{d} k_a p e \tan \delta + (1 - e) p$	$P_r$ = bearing capacity of the reinforced soil (Pa); $P_u$ = bearing capacity of unreinforced soil (Pa); $h/d$ = geocell aspect ratio (dimensionless); $k_a$ = coefficient earth pressure at rest (dimensionless); $p$ = load at the top of the geocell mattress (Pa); $e$ = stress redistribution effect (dimensionless) $\delta$ = interface shear angle between the cell wall and the filling soil (degrees)
Sitharam and Hegde [85]	Lateral resistance effect, vertical stress dispersion and membrane mechanisms	$P_r = P_u + 2P \tan^2(45 - \varphi/2) \tan \delta + P_r \left(1 - \frac{B}{B+2D_r \tan \beta}\right) + \frac{2T \sin \alpha}{B}$	$P_r$ = Bearing capacity of the geocell reinforced soil (kPa) $P_u$ = Bearing capacity of the unreinforced soil (kPa) $P$ = applied pressure on the geocell mattress (kPa) $\varphi$ = friction angle of the soil used to fill the geocell pockets (degrees) $\delta$ = interface shear angle between the cell wall and the filling soil (degrees) $B$ = footing width (m); $D_r$ = depth of the reinforcement (m) $\beta$ = load dispersion angle (degrees) $T$ = tensile strength of the basal geogrid material (kN/m) $\alpha$ = horizontal angle of the tensional force T (degrees) $B_g$ = width of the basal geogrid (m); $S$ = footing settlement measured at the surface (m).

in the study. Saride et al. [80] used the square shaped geocell pocket while modeling the multiple cell geocell in FLAC<sup>3D</sup>. The similar approach was also used by Leshchinsky and Ling [60] while modeling geocell reinforced ballast system in ABAQUS. However, the actual shape i.e. 3-D honeycomb shape) of the single cell geocell was modeled by Yang et al. [95], in their study. Hegde and Sitharam [40,41] made an attempt to model the real shape of the multiple cell geocells by considering the actual curvature of its pocket. In their study, the foundation soil, infill soil, and the geocell materials were assigned with three different material models to

simulate the real case scenario. A photograph of the single cell was taken and it was digitized to obtain the actual curvature of the cell. The co-ordinates were deduced from the curvature and the same were used in the FLAC<sup>3D</sup> to model the actual shape of the geocell [39]. Fig. 10b shows the typical numerical model of the geocells considering the actual shape. Table 7 presents the summary of the numerical studies on geocells.

Hegde and Sitharam [40] compared the vertical stress distribution below the footing for unreinforced and the geocell reinforced soils as shown in Fig 11a-b. In case of unreinforced bed, the

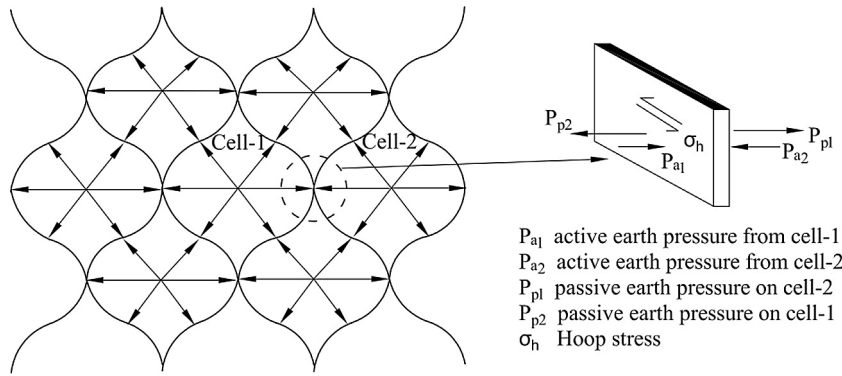


Fig. 8. Stresses in expanded geocells under compression loading (sourced from Hegde and Sitharam [38], with permission from ASCE).

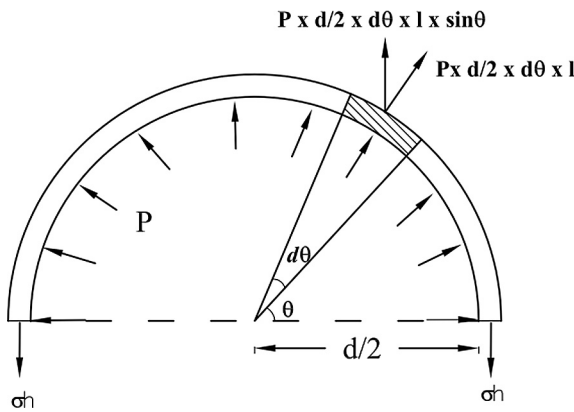


Fig. 9. Stresses acting on the surface of the geocell (sourced from Hegde and Sitharam [38], with permission from ASCE).

Table 6 Expressions for the calculation of stresses and strains on geocell surface.

Entity	Expression	Parameters
Hoop stress	$\sigma_h = \frac{P \times d}{2 \times t}$	$\sigma_h$ = Hoop stress on geocell $\epsilon_h$ = Hoop strain
Hoop strain	$\epsilon_h = \frac{P \times d \times (2 - \mu)}{4 \times t \times E}$	$P$ = active earth pressure exerted by the infill soil on the geocell wall $E$ = Yong's modulus;
Volumetric strain	$\epsilon_v = \frac{P \times d}{4 \times t \times E} (5 - 4\mu)$	$d$ = diameter of the geocell pocket; $\mu$ = Poisson's ratio; $t$ = thickness of the geocell

uniform pressure bulb of circular shape was observed. The pressure bulb was found to disperse up to the depth of  $1.6B$  (where  $B$  is the width of the footing). In geocell reinforced case, the pressure bulb of irregular shape was observed. However, the bulb was confined within geocell pocket and found to spread in lateral direction. The geocells distribute the load into the wider areas below the footing as compared to unreinforced bed [40].

6. Field performance

6.1. Case studies

Bush et al. [17] reported the construction of the geocell-reinforced embankments in soft clay in UK. Researchers had used the geocell of height 1 m with local soil as the infill material. With the geocells, about 33% lesser settlements were observed after 4

years when compared to systems with horizontal layers of reinforcement. Further, the cost savings of more than 31% were observed due to the provision of geocells. Cowland and Wong [19] presented the case history of the construction of the 10 m high road embankment supported on the geocell reinforced soft clay deposit. Two layers of the geocell mattress were used to support the two separate embankments of 300 m and 200 m long each. The geocell was coupled with the wick drains to support the embankment. In overall, the satisfactory performance of the geocell was observed in the project. Sitharam and Hegde [85] discussed the design and construction of the geocell supported embankment in soft settled red mud in Lanjigarh, Orissa in India. The consolidated red mud was having an average SPT-N value of 12. The embankment of 3 m height and 20 m wide and 680 m long was supported on the geocell foundation. Fig. 12 shows the schematic view of the geocell supported embankment in Lanjigarh. Over 15,000 m<sup>2</sup> of embankment base was stabilized using geocell foundation. The foundation work was completed within 15 days using locally available labours and the equipments. The excellent performance of the geocell was observed without any cracks, seepage or settlements in the embankments.

Emersleben and Meyer [27] reported the use of geocells in the reconstruction of the roads for a stretch of 500 m near the city of Hannover in Germany. The geocell was placed directly below the asphalt layer. Researchers evaluated the satisfactory performance of the geocells through various field tests. Kief et al. [56] presented the application of polyester based geocells in the pavement construction near Chennai, India. Researchers used the NPA geocells to reinforce the pavement section. Researchers opined that the geocells can be used in the upper pavement, directly under asphalt. Rajagopal et al. [78] reported the field performance of the geocell reinforced road section in India. The reported road section was constructed on the black cotton soil. Initially, the black cotton soil was treated with the lime and the geocell reinforcement of 150 mm thick was placed above the soil. The geocell pockets were filled with the good quality granular materials. As compared to the unreinforced road section in the same area, the geocell reinforced road sections maintained the uniform surface even after three seasons of heavy rainfall. Pokharel et al. [76] reported the use of the geocells in the construction of the unpaved roads in the region of northern Alberta and northern British Columbia. The Neoloy geocells of 150 mm height were used in these projects. A significant reduction in the rut depth was observed in the presence of geocells.

6.2. Field tests and large scale model tests

Emersleben and Meyer [27] conducted the field plate load tests and the falling weight deflectometer tests on the pavement rein-

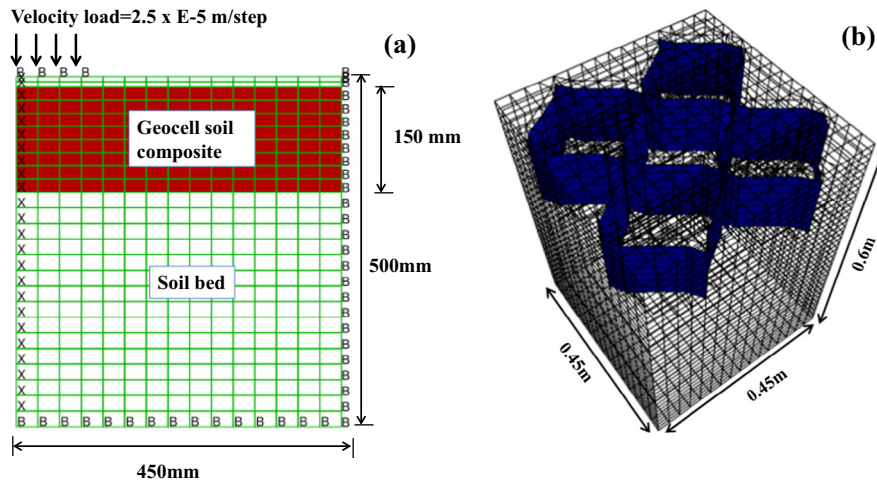


Fig. 10. Geocell model: (a) ECA approach; (b) actual shape of geocells (sourced from Hegde and Sitharam [39]).

Table 7

Summary of the numerical studies related to geocells.

Researchers	Approach adopted to model geocell	Software Programme	Type of study
Mhaiskar and Mandal [67]	ECA with Drucker-Prager model	3-D/ANSYS	Geocell reinforced clay bed with sand infill supporting rectangular footing
Bathurst and Knight [12]	ECA with Duncan-Chang model	2-D/GEOFEM	Geocell reinforced sand over steel conduit
Madhavi Latha and Rajagopal [66]	ECA with Mohr Coulomb model	2-D/GEOFEM	Geocell supported embankment on clay subgrade
Han et al. [29]	Square shape with Mohr Coulomb model for sand and linear elastic model for geocell	3-D/FLAC <sup>3D</sup>	Single cell supporting rectangular footing
Madhavi Latha et al. [64]	ECA with Duncan-Chang model	2-D/GEOFEM	Geocell reinforced sand supporting strip footing
Madhavi Latha et al. [65]	ECA with Duncan-Chang model	2-D/GEOFEM	Geocell reinforced sand supporting strip footing
Madhavi Latha and Somwanshi [66]	ECA with Duncan-Chang model	3-D/FLAC <sup>3D</sup>	Geocell reinforced sand supporting a square footing
Saride et al. [80]	Square shape with Mohr Coulomb model for clay and sand and linear elastic model for geocell	3-D/FLAC <sup>3D</sup>	Geocell reinforced clay supporting a circular footing
Yang et al. [95]	Honeycomb shape with Duncan-Chang model for sand and linear elastic model for geocell	3-D/FLAC <sup>3D</sup>	Single cell supporting circular footing
Hegde and Sitharam [32]	ECA with Mohr Coulomb model	2-D/FLAC <sup>2D</sup>	Geocell reinforced sand and clay bed supporting square footing
Hegde and Sitharam [36]	ECA with Mohr Coulomb model	2-D/FLAC <sup>2D</sup>	Geocell reinforced clay with different infill material
Hegde and Sitharam [38]	Circular shape with Mohr Coulomb model for infill material and linear elastic model for geocell	3-D/FLAC <sup>3D</sup>	Single cell supporting circular footing
Hegde and Sitharam [39]	Honeycomb shape with Mohr Coulomb model for sand and linear elastic model for geocell	3-D/FLAC <sup>3D</sup>	Geocell reinforced sand bed supporting square footing
Hegde and Sitharam [40]	Honeycomb shape with Modified Cam Clay for clay, Mohr Coulomb model for sand and linear elastic model for geocell	3-D/FLAC <sup>3D</sup>	Geocell reinforced clay bed supporting square footing

ECA = Equivalent Composite Approach.

forced with geocells. Researchers observed the 50% reduction in the vertical stress due to the provision of the geocell reinforcement. The falling weight deflectometer measurements revealed that the 15% reduction in the deflection of the road section. Han et al. [31] conducted the full scale moving load tests to evaluate the effect of geocell reinforcement on the recycled asphalt pavement (RAP). A test pit of dimension 6.1 m × 4.9 m × 1.8 m was dug and the subgrade consisted of the clay was prepared. Above the compacted subgrade, a layer of Neoloy Polymeric Alloy (NPA) geocell was placed and the cell pockets were filled with the RAP. Researchers observed that the geocell reinforcement improves the performance of unpaved RAP sections by widening the stress distribution angle and reducing the rut depth. Yang et al. [96] con-

ducted the accelerated pavement tests (APT) on the unpaved roads with geocell reinforced sand bases. Four sections of the unpaved roads were constructed at the APT facility of dimension 6.1 m × 4.9 m × 1.8 m made of concrete. Out of four sections, the two sections were unreinforced sections with aggregate cover at the top and the other two sections were geocell reinforced sections with different height of the geocell. Researchers observed the substantial reduction in the rut depth in the presence of geocells.

Tavakoli Mehrjardi et al. [89] carried out the full scale model tests to study the efficacy of the geocell reinforcement in protecting the buried pipeline under the action of repeated load. The tests were conducted in a concrete box of dimension 6.2 m × 2.5 m × 1.5 m. Test bed was prepared using the sandy soil

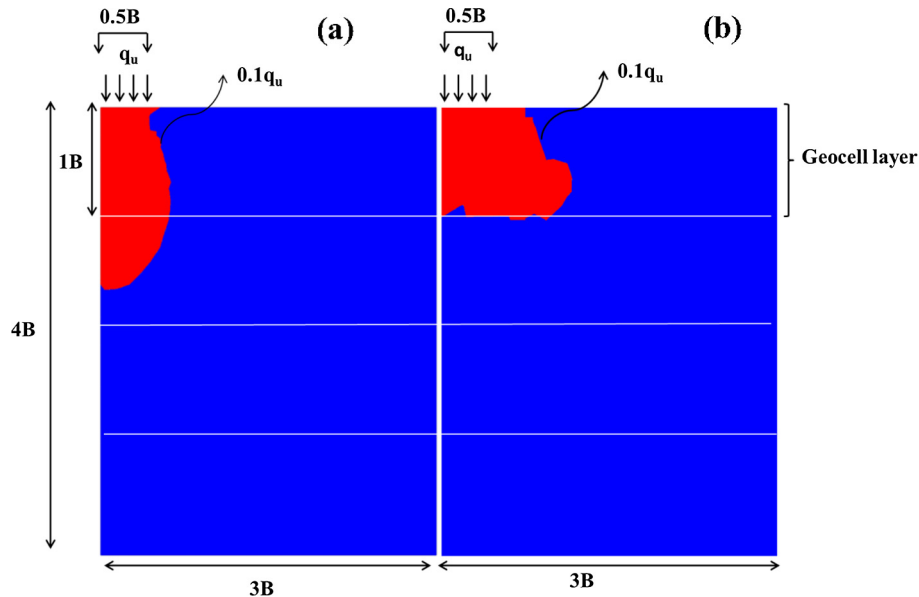


Fig. 11. Pressure bulbs corresponding to  $0.1q_u$ : (a) unreinforced; (b) geocell reinforced (sourced from Hegde and Sitharam [40]).

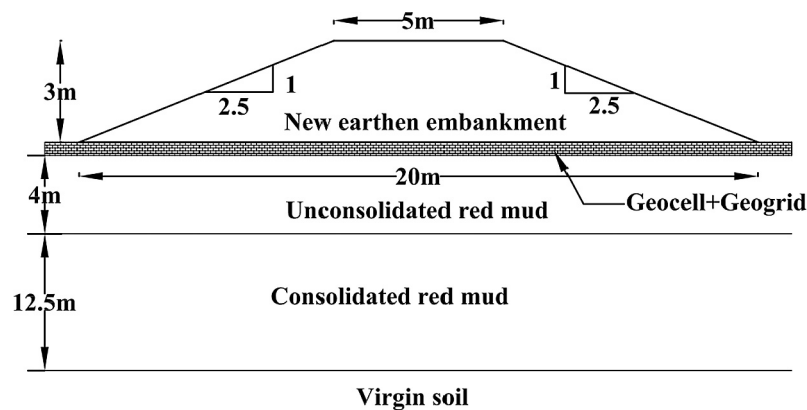


Fig. 12. Schematic representation of the geocell supported embankment (modified from Sitharam and Hegde [85]).

in their study. In the test bed, a trench of 0.5 m width was excavated and the PVC pipe of 160 mm diameter was placed. Repeated load was applied to the test bed with the help of a circular footing. Researchers observed the 35% reduction in the pipe strain in the presence of the geocell reinforcement as compared to unreinforced case. Tanyu et al. [88] carried out the series of large scale cyclic plate load tests on the geocell reinforced aggregate bases. Tests were conducted in a test facility with a  $3\text{ m} \times 3\text{ m} \times 3.5\text{ m}$  reinforced concrete pit. HDPE geocell was used in their study to reinforce the aggregate bases. Researchers observed the 30–50% reduction in the plastic deflection of the working platforms, 40–50% improvement in the resilient modulus of the subbase and 2 fold increment in the modulus of subgrade reaction of the bed due to the presence of geocells. Similarly, Moghaddas Tafreshi et al. [70] carried out a series of field cyclic plate load tests to assess the efficacy of the geocells in improving the performance of pavements. Tests were carried out in a pit of  $2\text{ m} \times 2\text{ m} \times 0.7\text{ m}$  using a 300 mm diameter rigid steel plate. Researchers observed that the use of the combined geocell and rubber soil mixture layers is more effective than geocell layers alone.

Apart from the load tests on the geocells, Guo et al. [28] carried out the outdoor field vegetation tests to investigate the effect of geosynthetic reinforcement on vegetation. Nowadays, in rural

areas, geocells have been used to stabilize the unpaved shoulders to accommodate temporary vehicle loads. However, there was a concern about the vegetation growth in such geocell reinforced sections. The test section of each  $1.5\text{ m} \times 1.5\text{ m}$  with different base and top soil combinations was prepared by reinforcing with the HDPE geocells. Perennial rye-grass seeds were planted and its growth was monitored up to a year. No evidence of geocell reinforcement limiting vegetation growth in unpaved shoulders was found in their study. Table 8 summarizes the previous studies related to field tests, large scale model tests and the case studies related to geocells.

## 7. Summary of the past studies

The majority of the past research studies has focused only on the geocell applications related to foundation engineering. Those investigations focused only on the quantification of the increase in bearing capacity of the soil due to the provision of the geocells. A very few researchers have focussed on developing the generalized design guidelines or the analytical solution scheme for the geocells. Unfortunately, many of these solution schemes are primitive and have major shortcomings. The review of the past studies

**Table 8**  
Field tests, large scale model tests and the case studies related to geocells.

Researchers	Type of soil	Type of geocell	Type of test	Application type	Test size /foot print area
<i>Field test/Large scale model tests</i>					
Emerleben and Meyer [27]	Soft soil	HDPE	Field plate load test	Pavements	2 m × 2 m × 2 m
Han et al. [31]	Clay	Neoloy Polymeric Alloy (NPA)	Moving wheel load tests	Pavement	6.1 m × 4.9 m × 1.8 m
Yang et al. [96]	Clay	Neoloy Polymeric Alloy (NPA)	Moving wheel load tests	Pavement	6.1 m × 4.9 m × 1.8 m
Tavakoli Mehrjardi et al. [89]	Sand	Non-woven geotextile cells	Large scale plate load test	Protection of buried pipeline	6.2 m × 2.5 m × 1.5 m.
Tanyu et al. [88]	Aggregates	HDPE	Large scale cyclic plate load test	Pavement	3 m × 3 m × 3.5 m
Moghaddas Tafreshi et al. [70]	Sand	Non-woven geotextile cells	Field cyclic plate load tests	Pavement	2 m × 2 m × 0.7 m
<i>Case studies</i>					
Cowland and Wong [19]	Soft clay	HDPE geogrid cells	N/A	Embankment	300 m × 200 m, 2 nos.
Sitharam and Hegde [85]	Red mud	Neoloy Polymeric Alloy (NPA)	N/A	Embankment	680 m × 20 m
Kief et al. [56]	Clay	Neoloy Polymeric Alloy (NPA)	N/A	Pavement	500 m

also suggests that a very few well documented case histories explaining the successful field applications of the geocells are available. Non-availability of the well documented case histories may indirectly affect the future field application of the geocells. The important issues related to the geocells such as effect of infill materials, stress distribution patterns, joint strength and wall deformation characteristics were not very well explored by the previous researchers. Except the foundations and embankments application of the geocells, the other applications were not very well explored. As there is a huge scope for the infrastructural growth in the 21st century, it is very high time to explore the new applications of geocells in geotechnical engineering.

## 8. Present research trends

This section summarizes the recent research development related to geocells. In the recent years, the research focus has shifted towards the understanding the response of the geocell under repeated and cyclic loading. It is due to the fact that the behaviour of the geocells under the cyclic loading is not clearly understood yet. Further, it has been found that the recent studies have targeted the new application areas of geocells such as railways, retaining walls, machine foundations, recycled asphalt pavements and protection of buried pipelines etc.

Moghaddas Tafreshi and Dawson [71] carried out the repeated load tests on the strip footing resting on the geocell reinforced sand beds. Geocell usage was found to reduce the plastic deformation under repeated loading. Similarly, Moghaddas Tafreshi et al. [70] highlighted the beneficial aspects of the geocells with the help of field cyclic plate load tests. Hegde and Sitharam [43] studied the behaviour of the square footing resting on the geocell reinforced soft clay geocell subjected to incremental cyclic loading. Researchers observed the significant improvement in the stiffness of the soil in the presence of the geocells. The geocell was found to improve the coefficient of elastic uniform compression the soil. Latha and Manju [59] carried out the seismic shake table tests on the geocell retaining wall. The retaining wall was subjected to base shaking of different magnitude and frequency. It was found that the geocell retaining walls were extremely strong to seismic shaking. The similar type of observations was also made by Ling et al. [61] based on the seismic shake table studies on the geocell retaining walls.

Nowadays, a substantial amount of recycled asphalt pavement (RAP) material is being produced from flexible pavement rehabilitation projects. RAP can be used as a base course material for sustain-

able pavement construction. Recent research studies have highlighted that the strength of the RAP bases can be increased using the geocell confinement (e.g. [31,91,92]). Han et al. [31] performed moving wheel tests on unpaved roads reinforced with geocells encasing the RAP. Researchers found that the geocell reduced the rut depth and vertical stress transferred to the subgrade. Bortz et al. [16] performed moving wheel tests on asphalt pavements with unreinforced and geocell reinforced bases. The performance of the geocell-reinforced RAP bases was found as good as the geocell reinforced well-graded aggregate base. Similarly, Thakur et al. [91] conducted large-scale laboratory cyclic plate loading tests on geocell-reinforced RAP bases over the weak subgrade. Researchers concluded that geocell improved the performance of RAP bases by reducing the permanent surface deformation and vertical stress at the interface of the base and subgrade. Thakur et al. [92] performed laboratory cyclic plate load tests on the geocell reinforced RAP bases resting on the weak and moderate subgrade. Researchers observed that the geocell confinement is more beneficial for the bases over the weak subgrade than those over the moderate subgrade.

The recent research works have also highlighted the beneficial use of the geocells in improving the rail track performance. The inclusion of synthetic materials to improve the rail track performance is relatively a new concept. Initially, the concept started with the use of the geotextiles and geogrid in the railway track (e.g. [48,49,50]). However, the recent trend is to reinforce the rail track with geocells. Lescenesky and Ling [60] have performed small scale dynamic plate load tests and 3D modelling studies to check the efficacy of the geocells in stabilizing the railway embankment. Results revealed that the presence of the geocell reduces the vertical and lateral deformation of the railway embankment system. Indraratna et al. [51] have performed small scale model tests to study the behaviour of the geocell reinforced subballast. Researchers observed that the geocell increases the confinement of the subballast system. Biabani et al. [13] studied the pull-out strength of the geocell reinforced railway subballast using the large scale model tests. The passive resistance of the track was found to increase in the presence of the geocells. Similarly, Biabani et al. [14] carried out the finite element simulation of the geocell reinforced subballast and opined that the confinement on the subballast increases due to geocells.

In addition to cyclic loading applications as discussed above, nowadays, the geocell is also gaining popularity in protection applications such as protection of buried pipelines and underground utilities. Underground conduits or utility pipelines form a

**Table 9**  
Geosynthetics for protection of buried pipelines.

Researchers	Type of soil	Pipe material	Pipe geometry	Reinforcement used
Moghaddas Tafreshi and Khalaj [72]	Sand	HDPE	110 mm dia and 4 mm thick	geogrid
Palmeira and Andrade [73]	Sand	Steel	75 mm dia and 1.5 mm thick	Combination of geotextile and geogrid
Tavakoli Mehrjardi et al. [90]	Sand	PVC	160 mm dia and 4 mm thick	Geocell with rubber soil-mixture
Tavakoli Mehrjardi et al. [89]	Sand	PVC	160 mm dia and 4 mm thick	Geotextiles and geocells in separately
Hegde and Sitharam [42,36–41]	Sand	PVC	75 mm dia and 1.4 mm thick	Geogrid, geocell and combination of both
Hegde et al. [34]	Clay	PVC	75 mm dia and 1.4 mm thick	Combination of geocell and geogrid

complex network in the urban areas and are often laid below the pavements and the temporary structures. Often, these conduits or pipelines are buried at shallow depths in trenches with the help of flowable fills [41]. Due to application of repeated traffic loads or heavy static loads from the vehicles, these pipes tend to deform and damage. The recent research suggests that the planar geosynthetics such as geotextiles and geogrids can be utilized to protect these pipelines e.g. [72,73]. Compared to planar geosynthetics, geocells are effective in reducing the vertical stress and the deformation on the pipelines [33,41,34]. The beneficial aspects of geocells in protecting the buried pipelines under static and repeated loads were also highlighted by Tavakoli et al., [90,89]. Table 9 summarizes the research activities related to the use of geosynthetics in the protection of buried pipelines.

## 9. Future prospects

Geocell is relatively a new material in geotechnical engineering in comparison with the conventional ground reinforcement techniques. The following enlists the future scope of research in the area of geocell confinement.

- The majority of the past studies conducted are small scale laboratory model tests. The existing theories and the modelling techniques are also derived from the laboratory model studies. The results of the small scale model tests are subjected to scale effects. Hence, more and more field tests or centrifuge model shall be conducted to ascertain the findings of the small scale model tests. It would be interesting to check the extent at which the full scale tests replicate the findings of the model studies.
- Many of the past studies are limited to static load applications of the geocells. The knowledge about the performance of the geocells subjected to cyclic loading are limited. There is a strong need to carry out the experiment and 3D numerical studies in this regard. This will help to extend the applications of the geocells into machine foundations, earthquake resistant designs and railway foundations etc.
- Not many case studies have been documented related to successful applications of the geocells. Systematic documentation of the more and more case histories is necessary to popularize the use of geocells.
- There is a strong need for the development of the robust design methodologies and analytical formulations related to geocells. These analytical formulations are required, particularly for estimating the bearing capacity and the settlement of the geocell reinforced foundation beds. Presently, there is no sophisticated methodology is available for the settlement calculation of the geocell reinforced soil.
- More and more realistic 3D-numerical simulations are required to understand the variation of the stresses and strains on the geocell surface. The close understanding of the geocell behaviour under the different types of load will helps to optimize the design of the geocells.

## 10. Conclusions

The use of geocells in various infrastructure projects has been attracting urban developers and contractors due to its various benefits. This paper reviewed the research activities related to geocell covering the wide spectrum of application. The main objective of this paper was to present the reader with the summary of the past studies, current state of art and the scope of the future research directions. The paper has discussed numerous studies related to geocells such as experimental, numerical, analytical and field performance. It was found from the previous studies that there exist several research gaps in the subject area, as indicated in the future scope of research. If these gaps are considered and studied, it can enhance the overall understanding of the geocell confinement. Further, it can lead to the development of design standards for geocell confinement systems. In overall, the past studies indicated that geocell is evolving as a ground reinforcement technique. In future, the geocells application will be more prominent in pavements, railways, foundations, RE walls and protection of the underground utilities.

## Acknowledgement

Author is thankful to Prof. T.G. Sitharam, Indian Institute of Science Bangalore for introducing him to the subject discussed in the manuscript.

## References

- [1] ASTM D5199, Standard Test Method for Measuring the Nominal Thickness of Geosynthetics, ASTM International, West Conshohocken, PA, 2012.
- [2] ASTM D5885, Standard Test Method for Oxidative Induction Time of Polyolefin Geosynthetics by High Pressure Differential Scanning Calorimetry, ASTM International, West Conshohocken, PA, 2015.
- [3] ASTM E831, Standard Test Method for Linear Thermal Expansion of Solid Materials by Thermomechanical Analysis, ASTM International, West Conshohocken, PA, 2014.
- [4] ASTM D3895, Standard Test Method for Oxidative-Induction Time of Polyolefins by Differential Scanning Calorimetry, ASTM International, West Conshohocken, PA, 2014.
- [5] ASTM E2254, Standard Test Method for Storage Modulus Calibration of Dynamic Mechanical Analysers, ASTM International, West Conshohocken, PA, 2013.
- [6] ASTM D1693, Standard Test Method for Environmental Stress-Cracking of Ethylene Plastics, ASTM International, West Conshohocken, PA, 2009.
- [7] ASTM D6992, Standard Test Method for Accelerated Tensile Creep and Creep-Rupture of Geosynthetic Materials based on Time-Temperature Superposition using the Stepped Isothermal Method, ASTM, West Conshohocken, PA, 2009.
- [8] ASTM D1505, Standard Test Method for Density of Plastics by the Density-Gradient Technique, ASTM International, West Conshohocken, PA, 2010.
- [9] J.O. Avesani Neto, B.S. Bueno, M.M. Futai, A bearing capacity calculation method for soil reinforced with a geocell, *Geosynthetics Int.* 20 (3) (2013) 129–142.
- [10] R.J. Bathurst, P.M. Jarrett, Large scale model tests of geo-composite mattresses over peat subgrades, *Transp. Res. Rec.* 1188 (1988) 28–36.
- [11] R.J. Bathurst, R. Karpurapu, Large scale triaxial compression testing of geocell reinforced granular soils, *Geotech. Test. J.* 16 (3) (1993) 296–303.
- [12] R.J. Bathurst, M.A. Knight, Analysis of geocell reinforced soil covers over large span conduits, *Comput. Geotech.* 22 (3/4) (1998) 205–219.
- [13] M.M. Biabani, N.T. Ngo, B. Indraratna, Performance evaluation of railway sub ballast stabilized with geocell based on pull-out testing, *Geotext. Geomembr.* 44 (2016) 579–591.

- [14] M.M. Biabani, B. Indraratna, N.T. Ngo, Modelling of geocell-reinforced sub ballast subjected to cyclic loading, *Geotext. Geomembr.* 44 (2016) 489–503.
- [15] J. Binquet, L.K. Lee, Bearing capacity tests on reinforced earth slabs, *J. Geotech. Eng. Div., ASCE* 101 (12) (1975) 1241–1255.
- [16] B.S. Bortz, M. Hossain, I. Halami, A. Gisi, Low-volume paved road improvement with geocell reinforcement, Transportation Research Board Annual Meeting Transportation Research Board, Washington, DC, 2012.
- [17] D.I. Bush, C.G. Jenner, R.H. Bassett, The design and construction of geocell foundation mattresses supporting embankments over soft ground, *Geotextile Geomembr.* 9 (1990) 83–98.
- [18] R.H. Chen, Y.W. Haung, F.C. Haung, Confinement effect of geocells on sand samples under triaxial compression, *Geotext. Geomembr.* 37 (2013) 35–44.
- [19] J.W. Cowland, S.C.K. Wong, Performance of a road embankment on soft clay supported on a geocell mattress foundation, *Geotext. Geomembr.* 12 (1993) 687–705.
- [20] S.K. Dash, N.R. Krishnaswamy, K. Rajagopal, Bearing capacity of strip footings supported on geocell-reinforced sand, *Geotext. Geomembr.* 19 (2001) 235–256.
- [21] S.K. Dash, K. Rajagopal, N.R. Krishnaswamy, Strip footing on geocell reinforced sand beds with additional planar reinforcement, *Geotext. Geomembr.* 19 (2001) 529–538.
- [22] S.K. Dash, S. Sireesh, T.G. Sitharam, Model studies on circular footing supported on geocell reinforced sand underlain by soft clay, *Geotext. Geomembr.* 21 (2003) 197–219.
- [23] S.K. Dash, K. Rajagopal, N.R. Krishnaswamy, Performance of different geosynthetic reinforcement material in sand foundations, *Geosynth. Int.* 11 (1) (2004) 35–42.
- [24] S.K. Dash, Influence of relative density of soil on performance of geocell reinforced sand foundations, *J. Mater. Civ. Eng.* 22 (5) (2010) 533–538.
- [25] S.K. Dash, Effect of geocell type on load carrying mechanism of geocell-reinforced sand foundations, *Int. J. Geomech.* 12 (5) (2012) 537–548.
- [26] J.M. Duncan, C.Y. Chang, Non-linear analysis of stress and strain in soils, *J. Soil Mech. Found. Div.* 96 (1970) 1629–1653.
- [27] A. Emersleben, N. Meyer, Bearing capacity improvement of gravel base layers in road constructions using geocells. Proceedings of 12th International conference of International Association for Computer Methods and Advances in Geomechanics (IACMG), 1–6 October, Goa, India (2008) 3538–3545.
- [28] J. Guo, J. Han, S.D. Schrock, R.L. Parsons, Field evaluation of vegetation growth in geocell-reinforced unpaved shoulders, *Geotext. Geomembr.* 43 (5) (2015) 403–411.
- [29] J. Han, X. Yang, D. Leshchinsky, R.L. Parsons, Behaviour of geocell reinforced sand under a vertical load, *J. Transp. Res. Board* 2045 (2008) 95–101.
- [30] J. Han, S.K. Pokhrel, R.L. Parsons, D. Leshchinsky, I. Halahmi, Effect of infill material on the performance of geocell-reinforced bases. Proceedings of 9th International Conference on Geosynthetics, Brazil, (2010) 1503–1506.
- [31] J. Han, S.K. Pokhrel, X. Yang, C. Manandhar, D. Leshchinsky, I. Halahmi, R.L. Parsons, Performance of geocell reinforced RAP bases over weak subgrade under full scale moving wheel loads, *J. Mater. Civ. Eng.* 23 (11) (2011) 1525–1534.
- [32] A. Hegde, T.G. Sitharam, Experimental and numerical studies on footings supported on geocell reinforced sand and clay beds, *Int. J. Geotech. Eng.* 7 (4) (2013) 346–354.
- [33] A. Hegde, S. Kadabnakatti, T.G. Sitharam, Protection of buried pipelines using a combination of geocell and geogrid reinforcement: experimental studies. *Geotechnical Special Publication 238, ASCE (Geo-Shanghai 2016)*, (2014) 289–298.
- [34] A. Hegde, S. Kadabnakatti, T.G. Sitharam, Use of geocells to protect buried pipelines and underground utilities in soft clayey soils. *Geotechnical Special Publication 271, ASCE (Geo-Chicago 2016)*, (2016) 914–924.
- [35] A. Hegde, Ground improvement using 3d-cellular confinement systems: experimental and numerical studies. (Ph.D. thesis) submitted to Indian Institute of Science Bangalore, India.
- [36] A. Hegde, T.G. Sitharam, Effect of infill materials on the performance of geocell reinforced soft clay beds, *Geomech. Geoenviron. Int. J.* 10 (3) (2015) 163–173.
- [37] A. Hegde, T.G. Sitharam, Use of bamboo in soft ground engineering and its performance comparison with geosynthetics: Experimental studies, *J. Mater. Civ. Eng. ASCE* 27 (9) (2015) 1–9.
- [38] A. Hegde, T.G. Sitharam, Joint strength and wall deformation characteristics of a single cell geocell subjected to uniaxial compression, *Int. J. Geomech. (ASCE)* 15 (5) (2015) 1–8.
- [39] A. Hegde, T.G. Sitharam, 3-dimensional numerical modelling of geocell reinforced sand beds, *Geotext. Geomembr.* 43 (2015) 171–181.
- [40] A.M. Hegde, T.G. Sitharam, 3-Dimensional numerical analysis of geocell reinforced soft clay beds by considering the actual geometry of geocell pockets, *Can. Geotech. J.* 52 (9) (2015) 1396–1407.
- [41] A. Hegde, T.G. Sitharam, Experimental and numerical studies on protection of buried pipelines and underground utilities using geocells, *Geotext. Geomembr.* 43 (2015) 372–381.
- [42] A. Hegde, T.G. Sitharam, Experimental and analytical studies on soft clay beds reinforced with bamboo cells and geocells, *Int. J. Geosynth. Ground Eng.* 1 (2) (2015) 1–13.
- [43] A. Hegde, T.G. Sitharam, Behaviour of geocell reinforced soft clay bed subjected to incremental cyclic loading, *Geomech. Eng.* 10 (4) (2016) 405–422.
- [44] A. Hegde, T.G. Sitharam, Experiment and 3D-numerical studies on soft clay bed reinforced with different types of cellular confinement systems, *Transp. Geotech.* 10 (2017) 73–84.
- [45] D.J. Henkel, G.D. Gilbert, The effect of the rubber membrane on the measured triaxial compression strength of clay samples, *Geotechnique* 3 (1) (1952) 20–29.
- [46] C.C. Huang, E. Tatsuoka, Prediction of bearing capacity in level sandy ground reinforced with strip reinforcement. Proceedings International Geotechnical Symposium on Theory and Practice of Earth Reinforcement, Balkema, Fukuoka, Kyushu, Japan, (1988) 191–196.
- [47] C.C. Huang, F. Tatsuoka, Bearing capacity of reinforced horizontal sandy ground, *Geotext. Geomembr.* 9 (1) (1990) 51–82.
- [48] B. Indraratna, H. Khabbaz, W. Salim, D. Christie, Geotechnical properties of ballast and the role of geosynthetics in rail track stabilization, *Ground Improvement* 10 (3) (2006) 91–101.
- [49] B. Indraratna, S. Nimbalkar, T. Neville, Performance assessment of reinforced ballasted rail track, *Ground Improvement* 167 (2013) 24–34.
- [50] B. Indraratna, S. Nimbalkar, Stress-Strain degradation response of railway ballast stabilized with geosynthetics, *Geotech. Geoenviron. Eng.* 139 (5) (2013) 684–700.
- [51] B. Indraratna, M.M. Biabani, S. Nimbalkar, Behaviour of geocell-reinforced subballast subjected to cyclic loading in plane-strain condition, *J. Geotech. Geoenviron. Eng.* 141 (1) (2015) 04014081.
- [52] ISO 11357 (2006). Determination of oxidation induction time of a polyolefin, Geneva.
- [53] ISO 6721-1 (2011). Plastics-Determination of dynamic mechanical properties. Part 1: General principles, Geneva.
- [54] ISO 11359-2 (1999). Determination of coefficient of linear thermal expansion and glass transition temperature. Geneva.
- [55] N. Janbu, Soil compressibility as determined by odometer and triaxial tests, European Conference on Soil Mechanics and Foundation Engineering, Wiesbaden, Germany, 1 (1963) 19–25.
- [56] O. Kief, K. Rajagopal, A. Rajagopal, S. Chandramouli, Modulus improvement factor for geocell-reinforced bases. *Geosynthetics India-11*, Chennai, India, 2011.
- [57] N.R. Krishnaswamy, K. Rajagopal, G. Madhavi Latha, Model studies on geocell supported embankments constructed over a soft clay foundation, *Geotech. Testing J. ASTM* 23 (2) (2000) 45–54.
- [58] R.M. Koerner, *Designing with Geosynthetics*, Prentice Hall, New Jersey, 1998.
- [59] G.M. Latha, G.S. Manju, Seismic response of geocell retaining walls through shaking table tests, *Int. J. Geosynth. Ground Eng.* (2016), <http://dx.doi.org/10.1007/s40891-016-0048-4>.
- [60] B. Leshchinsky, H. Ling, Effects of geocell confinement on strength and deformation behaviour of gravel, *J. Geotech. Geoenviron. Eng.* 139 (2) (2013) 340–352.
- [61] H. Ling, D. Leshchinsky, J. Wang, Y. Mohri, A. Rosen, Seismic response of geocell retaining walls: experimental studies, *J. Geotech. Geoenviron. Eng.* 135:4(515) (2009), 515–524. doi: 10.1061/(ASCE)1090-0241(2009).
- [62] G. Madhavi Latha, Investigations on the behaviour of Geocell supported embankments (Ph.D. thesis), Indian Institute of Technology, Madras, India, 2000.
- [63] G. Madhavi Latha, K. Rajagopal, Parametric finite element analyses of geocell-supported embankment, *Can. Geotech. J.* 44 (8) (2007) 917–927.
- [64] G. Madhavi Latha, S.K. Dask, K. Rajagopal, Equivalent continuum simulations of geocell reinforced sand beds supporting strip footings, *Geotech. Geol. Eng.* 26 (2008) 387–398.
- [65] G. Madhavi Latha, S.K. Dask, K. Rajagopal, Numerical simulation of the behaviour of geocell reinforced sand foundations, *Int. J. Geomech.* 9 (4) (2009) 143–152.
- [66] G. Madhavi Latha, A. Somwanshi, Effect of reinforcement form on the bearing capacity of square footing on sand, *Geotext. Geomembr.* 27 (2009) 409–422.
- [67] S.Y. Mhaiskar, J.N. Mandal, Investigations on soft clay subgrade strengthening using geocells, *Constr. Build. Mater.* 10 (4) (1996) 281–286.
- [68] J.N. Mandal, P. Gupta, Stability of geocell-reinforced soil, *Constr. Build. Mater.* 8 (1) (1994) 55–62.
- [69] Iman Mehdipour, Mahmoud Ghazavi, R.Z. Moayed, Numerical study on stability analysis of geocell reinforced slopes by considering the bending effect, *Geotext. Geomembr.* 37 (2013) 23–34.
- [70] S.N. Moghaddas Tafreshi, O. Khalaj, A.R. Dawson, Repeated loading of soil containing granulated rubber and multiple geocell layers, *Geotext. Geomembr.* 42 (2014) 25–38.
- [71] S.N. Moghaddas Tafreshi, A.R. Dawson, Behaviour of footings on reinforced sand subjected to repeated loading comparing use of 3D and planar geotextile, *Geotext. Geomembr.* 28 (2010) 434–447.
- [72] S.N. Moghaddas Tafreshi, O. Khalaj, Laboratory tests of small-diameter HDPE pipes buried in reinforced sand under repeated load, *Geotext. Geomembr.* 26 (2008) 145–163.
- [73] E.M. Palmeira, H.K.P.A. Andrade, Protection of buried pipes against accidental damage using geosynthetics, *Geosynth. Int.* 17 (4) (2010) 228–241.
- [74] Presto, Geoweb Load Support System – Technical Overview, Presto Products Company, Appleton, WI, USA, 2008.
- [75] S.K. Pokharel, J. Han, D. Leshchinsky, R.L. Parsons, I. Halahmi, Investigation of factors influencing behaviour of single geocell reinforced bases under static loading, *Geotext. Geomembr.* 28 (6) (2010) 570–578.
- [76] S.K. Pokharel, I. Martin, M. Norouzi, M. Breault, Validation of geocell design for unpaved roads. Proceedings of Geosynthetics 2015, February 15–18, Portland, Oregon, 2015.

- [77] K. Rajagopal, N.R. Krishnaswamy, G. Madhavi Latha, Behaviour of sand confined with single and multiple geocells, *Geotext. Geomembr.* 17 (1999) 171–181.
- [78] K. Rajagopal, S. Chandramouli, A. Parayil, K. Iniyar, Studies on geosynthetic-reinforced road pavement structures, *Int. J. Geotech. Eng.* 8 (3) (2014) 287–298.
- [79] C. Rea, J.K. Mitchell, Sand reinforcement using paper grid cells. ASCE Spring Convention and Exhibit, Preprint 3130, Pittsburgh, PA, April, 24–28, 1978.
- [80] S. Saride, S. Gowrisetti, T.G. Sitharam, A.J. Puppala, Numerical simulations of sand and clay, *Ground Improvement* 162 (G14) (2009) 185–198.
- [81] S. Sireesh, T.G. Sitharam, S.K. Dash, Bearing capacity of circular footing on geocell sand mattress overlying clay bed with void, *Geotext. Geomembr.* 27 (2) (2009) 89–98.
- [82] T.G. Sitharam, S. Sireesh, Model studies of embedded circular footing on geogrid reinforced sand beds, *Ground Improvement* 8 (2) (2004) 69–75.
- [83] T.G. Sitharam, S. Sireesh, Behaviour of embedded footings supported on geocell reinforced foundation beds, *Geotech. Test. J. ASTM* 28 (5) (2005) 452–463.
- [84] T.G. Sitharam, S. Sireesh, Effects of base geogrid on geocell-reinforced foundation beds, *Geomech. Geoeng. Int. J.* 1 (3) (2006) 207–216.
- [85] T.G. Sitharam, A. Hegde, Design and construction of geocell foundation to support embankment on soft settled red mud, *Geotext. Geomembr.* 41 (2013) 55–63 (Impact factor 2.38).
- [86] E. Schlosser, H.M. Jacobsen, I. Juran, Soil reinforcement: general report. 8th European Conference on Soil Mechanics and Foundation Engineering, Balkema, Helsinki, (1983) 83–103.
- [87] J. Takemura, M. Okamura, N. Suesmasa, T. Kimura, Bearing capacity and deformations of sand reinforced with geogrids. Proceedings of Earth Reinforcement Practice, Balkema, Fukuoka, Kyushu, Japan, (1992) 695–700.
- [88] B.F. Tanyu, A.H. Aydilek, A.W. Lau, T.B. Edil, C.H. Benson, Laboratory evaluation of geocell-reinforced gravel subbase over poor subgrades, *Geosynth. Int.* 20 (2) (2013) 47–61.
- [89] Gh. Tavakoli Mehrjardi, S.N. Moghaddas Tafreshi, A.R. Dawson, Pipe response in a geocell-reinforced trench and compaction considerations, *Geosynth. Int.* 20 (2) (2013) 105–118.
- [90] Gh. Tavakoli Mehrjardi, S.N. Moghaddas Tafreshi, A.R. Dawson, Combined use of geocell reinforcement and rubber soil mixtures to improve performance of buried pipes, *Geotext. Geomembr.* 34 (2012) 116–130.
- [91] J.K. Thakur, J. Han, S.K. Pokharel, R.L. Parsons, Performance of geocell-reinforced recycled asphalt pavement (RAP) bases over weak subgrade under cyclic plate loading, *Geotext. Geomembr.* 35 (2012) 14–24.
- [92] J. Thakur, J. Han, R. Parsons, Factors influencing deformations of geocell-reinforced recycled asphalt pavement bases under cyclic loading, *J. Mater. Civ. Eng.* (2016), [http://dx.doi.org/10.1061/\(ASCE\)MT.1943-5533.0001760](http://dx.doi.org/10.1061/(ASCE)MT.1943-5533.0001760).
- [93] S.G. Thallak, S. Saride, S.K. Dash, Performance of surface footing on geocell-reinforced soft clay beds, *J. Geotech. Geol. Eng.* 25 (2007) 509–524.
- [94] X. Yang, J. Han, Analytical model for resilient modulus and permanent deformation of geosynthetic-reinforced unbound granular material, *J. Geotech. Geoenviron. Eng.* 139 (9) (2013) 1443–1453.
- [95] X. Yang, J. Han, R.L. Parsons, D. Leshchinsky, Three-dimensional numerical modelling of single geocell reinforced sand, *Front. Archit. Civ. Eng. China* 4 (2) (2010) 233–240.
- [96] X. Yang, J. Han, S.K. Pokharel, C. Manandhar, R.L. Parsons, D. Leshchinsky, I. Halahmi, Accelerated pavement testing of unpaved roads with geocell reinforced sand bases, *Geotext. Geomembr.* 32 (2012) 95–103.
- [97] M.X. Zhang, A.A. Javadi, X. Min, Triaxial tests of sand reinforced with 3D inclusions, *Geotext. Geomembr.* 24 (2006) 201–209.
- [98] M.H. Zhao, L. Zhang, X.J. Zou, H. Zhao, Research progress in two direction composite foundation formed by geocell reinforced mattress and gravel piles, *Chin. J. Highway Transp.* 22 (1) (2009) 1–10.
- [99] L. Zhang, M. Zhao, C. Shi, H. Zhao, Bearing capacity of geocell reinforcement in embankment engineering, *Geotext. Geomembr.* 28 (2010) 475–482.